atmosphere

MDPI

Article

Temporal Variability of Equivalent Black Carbon Components in Atmospheric Air in Southern Poland

Natalia Zioła [1,2,*], Barbara Błaszczak [1] and Krzysztof Klejnowski [1]

[1] Institute of Environmental Engineering of the Polish Academy of Sciences, 34 M. Skłodowska-Curie Str., 41-819 Zabrze, Poland; barbara.blaszczak@ipis.zabrze.pl (B.B.); krzysztof.klejnowski@ipis.zabrze.pl (K.K.)
[2] Institute of Earth Sciences, Faculty of Natural Sciences, University of Silesia, Bankowa 12, 40-007 Katowice, Poland
* Correspondence: natalia.ziola@ipis.zabrze.pl; Tel.: +48-322-716-481

Abstract: This study assesses the air quality in Zabrze (southern Poland) based on the ambient concentrations of equivalent black carbon (eBC). eBC measurement campaigns were carried out from April 2019 to March 2020 using a modern AE33 Aethalometer, accompanied by parallel measurements of gaseous pollutants, PM_{10} and meteorological parameters. The use of the two-component AE33 model allows for the determination of the eBC from fossil fuel combustion (eBC_{ff}) and biomass burning (eBC_{bb}). The obtained results showed a clear seasonal variability of eBC concentrations, with higher average levels in the heating season (4.70 $\mu g \cdot m^{-3}$) compared to the non-heating one (1.79 $\mu g \cdot m^{-3}$). In both seasons, the eBC_{ff} component had a dominant share in total eBC, which indicates significant emissions from the combustion of fossil fuels for heating purposes and from local traffic sources. The obtained results showed high correlation coefficients with gaseous and particulate pollutants, with the strongest relationship for eBC and carbon monoxide (CO). During the non-heating and heating period, both anticyclone and cyclone systems played an important role in shaping eBC, eBC_{ff} and eBC_{bb} concentrations. High concentrations of all components occurred with a significant decrease in air temperature and solar radiation in winter.

Keywords: black carbon; soot; carbonaceous matter; fossil fuels; biomass burning; soot; Aethalometer; meteorology; Southern Poland

Citation: Zioła, N.; Błaszczak, B.; Klejnowski, K. Temporal Variability of Equivalent Black Carbon Components in Atmospheric Air in Southern Poland. *Atmosphere* **2021**, *12*, 119. https://doi.org/10.3390/atmos12010119

Received: 14 October 2020
Accepted: 13 January 2021
Published: 15 January 2021

1. Introduction

Atmospheric aerosols are receiving increasing attention in scientific research primarily due to their importance in influencing climate, restricting visibility, and causing harmful effects on human health and ecosystem stability [1–3]. One of the most important components of atmospheric aerosols is a carbonaceous component which can be in the range of about 20–45% of $PM_{2.5}$ (particles with aerodynamic diameter dae $\leq$ 2.5 µm) and slightly less (20–35%) of PM_{10} (dae $\leq$ 10 µm), on an annual basis [4,5].

The carbon fraction exists in aerosols in many different chemical and physical forms, and its total content in particulate matter, total carbon (TC) can be determined by elemental analysis. A specific subset of aerosol carbon—generally a small fraction of aerosol TC—is called e.g., black carbon (BC) or elemental carbon (EC). In reality, however, such a homogeneous fraction does not exist because it cannot be uniquely separated from organic carbon by any method [6]. The difference between EC and BC concerns the analytical method used to evaluate their content. The term EC is based on thermal methods, while BC refers to the optical properties of aerosol particles which are determined by optical methods [7]. In the optical method, the mass concentration of BC is obtained indirectly from light attenuation measurements; therefore, the term of equivalent black carbon (eBC) should be used [2]. However, in the literature, both definitions are found in the part concerning the results obtained from the optical method [8,9]. Black carbon (BC) is the

most important light-absorbing aerosol that is co-emitted with another important fraction called brown carbon (BrC) [10,11].

Brown carbon is often a by-product of biomass burning and is distinguished by its preference to absorb at near-UV wavelengths while the interference of brown carbon or mineral dust in the red and near-infrared wavelengths is minimal [12–15]. The recent discovery of the presence of BrC raises a lot of controversy because it may severely bias measurements of BC vast parts of the troposphere, especially those strongly polluted by biomass burning, where the mass concentration of brown carbon is high relative to that of black carbon. For this reason, it is extremely important to confirm the presence of brown carbon and its quantitative determination in order to recognize the BC as a precisely defined and well-determined unit in the entire troposphere; however, this fact is commonly omitted in black carbon monitoring [13].

The carbonaceous substance contained in atmospheric dust is of great importance due to its properties. First of all, the direct impact of the carbonaceous fraction on the Earth's natural energy balance should be emphasized [16–19]. Black carbon absorbs solar radiation over a wide range of wavelengths. Due to such specific properties, BC is considered to be one of the factors associated with the problems of global warming [2,18,19]. BC can also influence the climate indirectly. This component affects cloud albedo by changing the hygroscopicity of cloud condensation nuclei, which in turn can lead to changes in cloudiness and precipitation rates [20–22]. Being chemically inert and concentrated in submicron-sized particles, BC has a long atmospheric lifetime (of several days to weeks) and hence—with favorable atmospheric conditions such as no precipitation—can be subject to long-range transport processes [1,17,23,24]. Transported BC particles can accumulate on a surface covered with snow or ice, and therefore can contribute to accelerating the melting of glaciers by increasing the temperature of their surface [25]. In addition to various climate impacts, BC has adverse effects on terrestrial and aquatic ecosystems [26] as well as on public health [27]. Due to their submicron size, BC particles can penetrate deep into the human respiratory system, causing both physical and chemical interactions with lung tissues [28,29]. The chemical interactions are the result of a highly developed surface of BC particles, where the sorption of harmful substances occurs, e.g., heavy metals and polycyclic aromatic hydrocarbons (PAHs).

The harmful effect of black carbon on the climate, environment, and human health makes it an important parameter shaping the air quality. Black carbon is emitted only as a primary pollutant, and its formation occurs as a result of incomplete combustion of biomass and fossil fuels [30–32]. BC sources in urban areas are usually dominated by anthropogenic activities, such as transportation, industry, and residential combustion [2,33]. It has been estimated that, globally, 24% and 60% of anthropogenic BC emissions are from transport and residential combustion sources, respectively [33]. The high health risk of urban residents associated with exposure to BC and other air pollutants is also affected by compact urban buildings, which impede horizontal air ventilation [34,35]. The influence of local meteorological conditions—air temperature, relative humidity, atmospheric pressure, wind speed and direction—which determine the transport of substances in atmospheric air is not without significance [22]. Moreover, atmospheric circulation is also important, and some authors have shown that it is a better predictor of the weather impact on health than a single meteorological variable [36].

Growing urbanization is associated with an increase in the volume of traffic in cities, the intensification of industry, and the intensive burning of fossil fuels and biomass. Despite the substantial spatial and temporal variability in the BC emissions, the decline in the significance of vehicular traffic—due to technology advancements and legislation—is generally observed. On the other hand, the role of residential combustion, which is not currently regulated in most European countries, is increasing [33,37]. Although eBC is not covered by air quality standards, it has been recognized as an important parameter in the tools used to manage air quality in cities [38–40]. It is important to continue BC measurements and improve monitoring techniques, especially in areas such as southern

Poland, where numerous anthropogenic sources are located which lead to an overall high level of air pollution. The use of modern automatic equipment—like aethalometers—allows for obtaining results in high time resolution and estimating the different sources of eBC [32,41–45].

Taking into account the above considerations, a year-long measurement campaign of eBC concentrations from the urban area of Zabrze was examined for assessment of daily and seasonal variations. The southern region of Poland is one of the most polluted regions in Europe in terms of air quality due to the impact of numerous small and large-scale industries, low-level emission sources, and high vehicular density [46]. By analyzing the quantitative distribution of eBC in two different seasons (heating/non-heating), the impact of local sources and meteorological parameters in the intensity of pollutant emissions from anthropogenic sources on air quality in southern Poland was determined.

Moreover, the use of the modern AE33 Aethalometer allowed estimating the amount of eBC from the combustion of fossil fuels (eBC_{ff}) and biomass (eBC_{bb}). In addition, the work includes the impact of selected gaseous pollutants as well as meteorological conditions and air circulation types on the eBC concentration course. The results obtained as part of the work will enhance the existing knowledge about the status of black carbon in urban areas. On the other hand, understanding the origin sources of BC could provide tools for improving decision-making, including city planning and relevant source emission restrictions.

2. Materials and Methods

2.1. Study Area

eBC and meteorological parameters were measured in Zabrze (50.3° N, 18.7° E) localized within the Silesia Province (southern Poland) (Figure 1a) from 1 April 2019 to 31 March 2020. The measurements covered two periods: non-heating (1 April–30 September 2019) and heating (1 October 2019–31 March 2020) season. The measurement site met the requirements for urban background locations [47] and was situated in the area belonging to the Institute of Environmental Engineering Polish Academy of Sciences (IEE PAS). Figure 1b shows that the immediate surroundings of the measuring point are mainly residential buildings and houses—connected to the central heating network or heated by coal-fired boilers—as well as allotment gardens. The nearest road with high traffic intensity is located at a distance of about 300 m from the sampling site.

2.2. Instrumentation and Data Sources

eBC mass concentrations were monitored continuously using an automated measuring device—a modern Aethalometer AE33 (see Section 2.3)—located on the roof of the Institute's building (6 m above the ground). To assess the utility of the eBC source from the AE33, we derived the fossil fuels combustion (eBC_{ff}) and biomass-burning (eBC_{bb}) contributions to total eBC. Data on concentrations of selected gaseous (SO_2, NO_2, NO_x, NO, O_3, CO) and particulate (PM_{10}) pollutants were obtained from the Regional Inspectorate for the Environmental Protection (RIEP) database [48]. RIEP measurements were carried out at a station approximately 70 m from the IEE PAS. The sampling site of the Institute was also equipped with a meteorological station, thanks to which the basic meteorological parameters (air temperature, humidity, pressure, solar radiation) were measured in parallel with eBC measurements. For the assessment of probable source regions of eBC, climatological daily statistics were used. They specify the so-called types of circulation—the adopted parameterization based on the analysis of selected parameters of meteorological fields and the location of baric systems. The classification of circulation types according to Niedźwiedź [49] was used in the study. It is similar to the known British typology of Lamb [50] and includes 21 types of circulation—including 10 cyclonal and 10 anticyclonal (see Table 1). In addition, the classification of circulation types by Niedźwiedź [49] also includes dominant directions of air advection (16 types), as well as types without the direction of advection (Ca, Ka, Cc, Bc).

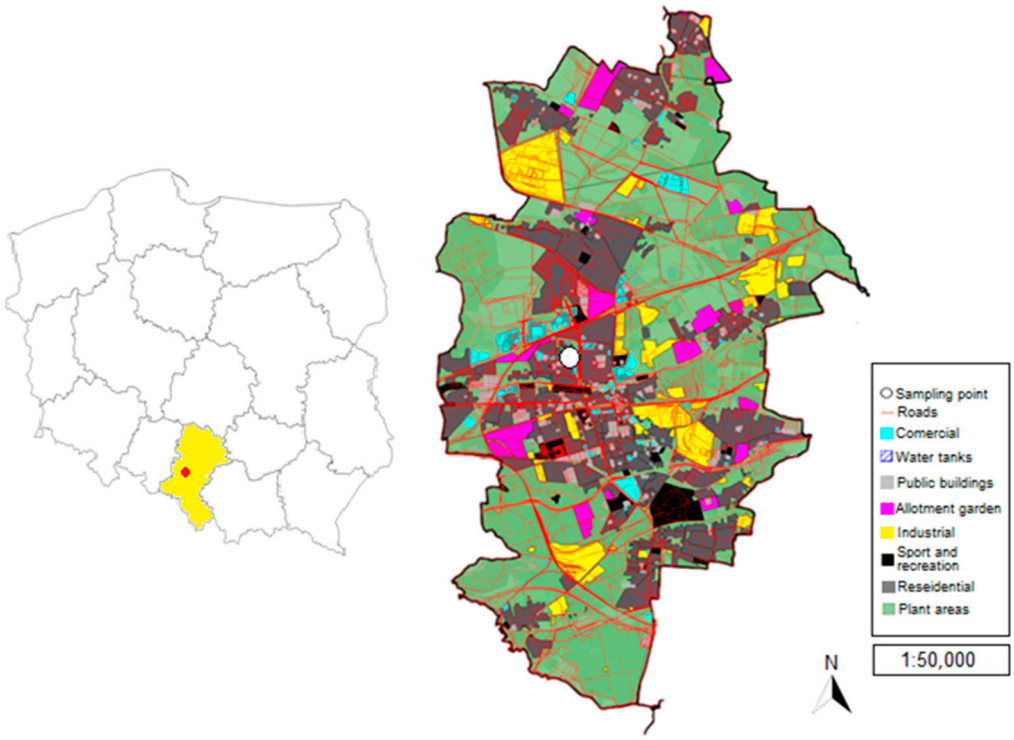

(**a**) (**b**)

Figure 1. The location of the sampling point (50.3° N, 18.7° E) shown on the map of Poland with the Silesian voivodeship marked (**a**) and with an indication of the specified land development in Zabrze (**b**). (The land development map was made using the generally available QGIS 3.6.3 software).

Table 1. A list of the atmospheric circulation types according to Niedźwiedź (2017).

Type of Circulation	Explanation
Na (1), Nc (11)	Situations with advection from the north
NEa (2), NEc (12)	Situations with advection from the northeast
Ea (3), Ec (13)	Situations with advection from the east
SEa (4), SEc (14)	Situations with advection from the southeast
Sa (5), Sc (15)	Situations with advection from the south
SWa (6), SWc (16)	Situations with advection from the southwest
Wa (7), Wc (17)	Situations with advection from the west
NWa (8), NWc (18)	Situations with advection from the northwest
Situations without a specific direction of advection	
Ca (9)	Central anticyclone situation (high center)
Ka (10)	Anticyclonic wedge or ridge of high pressure
Cc (19)	Central cyclonic, center of low
Bc (20)	Through of low pressure (different directions of air flow and frontal system in the axis of through)
x (21)	Unclassified situations or pressure col

a—anticyclonic situation; c—cyclonic situation.

2.3. Aethalometer AE33

The Aethalometer AE33 (Magee Scientific) is a high-sensitivity automatic measuring device designed for continuous measurements of the light absorption by BC particles. This apparatus has been commonly used in numerous research studies regarding the assessment of equivalent BC content in atmospheric air [32,51–54]. During operation of the device, the air stream with a volume of 5 $L \cdot m^{-1}$ was passed through a point on the filter tape made of

TFE-coated glass fiber (no. M8020). The inlet cut-off size was 1 µm (sharp cut cyclone, BGI model SCC1.197) and the measurement time resolution was set to 10 s.

The AE33 calculates light attenuation (ATN) due to particle deposit on the filter relative to a clean part of the filter, called the reference point—Equation (1) [52–55]:

$$ATN = 100 \cdot \ln(I_0/I) \quad (1)$$

where: I—signal from the point with the sample; I_0—signal from the reference point. The mass concentration is determined by measuring the rate of change in light attenuation assumed due solely to absorption by BC. It should be noted that the result is a mathematical combination of a measurement carried out simultaneously at two aerosol-loaded points with two different flows and at a reference point without flow. Measurements at two points with aerosol are necessary due to the filter loading artifacts, resulting from the deposition of aerosol particles on the filter tape. In order to measure the filter load and calculate the compensation parameter, a real-time compensation algorithm was developed for the AE33 device. In turn, the attenuation factor is determined based on the modification of the light attenuation as a function of time, volume flow rate and filter surface area [52,54].

In the case of AE33, aerosol light absorption was measured at seven different wavelengths (λ) from near-ultraviolet to near-infrared (λ = 370, 470, 520, 590, 660, 880, and 950 nm). The total BC mass concentration (or eBC) is here reported at a wavelength of 880 nm (channel 6) because other particles—e.g., mineral dust—absorb light at this wavelength to a much lesser extent [45]. The use of the multi-wavelengths AE33 allows us to estimate the effects of the combustion of fossil fuels (eBC_{ff}) and biomass burning (eBC_{bb}) on the total BC mass. Aerosols from fossil fuel sources (assuming light absorption mostly by BC) can efficiently absorb solar radiation from the near ultraviolet (UV) throughout the visible and to the near-infrared (IR) wavelengths almost inversely proportional to the wavelength, while aerosols from biomass burning sources (light absorption by both BC and BrC) may absorb relatively more at the near-UV than at the IR (predicted by the inverse wavelength dependence). This relationship (absorption vs. wavelength) is represented by the Angstrom Absorption Exponent (AAE) [15,55,56].

This assumption is the basis of the built-in Aethalometer model [57,58] which assumes that the total light-absorbing sample (b_{abs_total}) is determined by two types of light-absorbing particles—from fossil fuels combustion (b_{abs_ff}) and biomass burning (b_{abs_bb}):

$$B_{abs\_total} = B_{abs\_ff} + B_{abs\_bb} \quad (2)$$

The basis of the presented Aethalometer model are the values of the absorption exponent Ångström (α), which on the basis of several emission measurements was determined for BC from the fossil fuels combustion and biomass burning. For example, Sandradewi et al. (2008) suggested that α_{ff} was 1.1 and α_{bb} was 1.8–1.9 from the light absorption at 470 and 950 nm. The a priori assumptions of Ångström absorption for both sources are therefore the basis for determining both sources in the Aethalometer model.

Although the Aethalometer model is widespread, there are some uncertainties related to the adoption of constant parameters to determine the share of BC mass concentration from fossil fuel combustion and biomass burning. For this reason, along with the measurements with AE33, measurements should be made with the reference method, e.g., the radiocarbon (14C) method, because it allows for the validation of the selection of absorption exponents for fossil fuels combustion and biomass burning, which should be assumed a priori in the Aethalometer model [59]. In addition, reference methods are used simultaneously with AE33 measurements [60], which question the usefulness of the Aethalometer model due to additional combustion sources (BrC) that can significantly affect the mass concentration of BC from the above sources.

In the absence of standard reference material, it is recommended to report the aerosol light absorption coefficient, which eliminates the uncertainty resulting from adopting a specific mass-specific absorption coefficient (MAC). When reporting to the eBC, it is crucial

to identify the MAC value used for the conversion and to define the approach used to separate the potential contribution of BrC or mineral dust to the aerosol light absorption coefficient [61].

The results of previous studies show that the reference method for the determination of absorption exponents for fossil fuels combustion and biomass burning is important and should be performed using the Aethalometer model. However, when the reference method is not used, the assumption of one set of absorption exponents gives acceptable results and the BC apportionment by sources should only be interpreted qualitatively [59].

As mentioned in many scientific articles [10,13,15], it should be remembered that aerosols from biomass combustion, apart from BC, may contain a significant part of organic substances absorbing ultraviolet radiation (the so-called brown carbon—BrC). Accurate separation of BCbb from BrC is complex and requires additional methodological improvements or a parallel measurement of indicator compounds, such as Levoglucosan, which was not done in this study. Undoubtedly, this fact should be taken into account in future scientific research. However, this will not significantly affect the assessment of the impact of these two groups of sources on the degree of air pollution with carbon aerosol, and the results should be treated in terms of the quality assessment of the atmospheric air in Zabrze.

2.4. Data Processing and Statistical Analyses

In order to document the results of measurements of eBC and its two components eBC_{bb}, eBC_{ff} concentrations, as well as concentrations of other particulate and gaseous pollutants, a source database was prepared in the MsExcel 2013 spreadsheet. With regard to the data obtained from the RIEP website, the database included 1-h averaged concentrations of SO_2, NO_2, NO_x, NO, O_3, CO, and PM_{10}. In the case of the total eBC and its components (eBC_{ff} and eBC_{bb}), the database was a set of raw data recorded by the AE33 over a period of 10 s. On their basis, the mean 1-h concentrations were further calculated, which were used to obtain the mean daily mass concentrations (Section 3.1) and to prepare graphs of the monthly-diurnal variations of the mass concentrations of eBC, eBC_{bb}, and eBC_{ff} (Section 3.2).

Before proceeding to statistical analysis, the measurement results carried out in the period from 1 January 2019 to 31 March 2020 were subject to initial verification based on the provisions of Directive 2008/50/EC regarding data quality objectives, especially the required proportion of valid data, which is 75% or 90%, respectively, when the hourly/daily and annual mean concentrations are estimated. These criteria were also applied to concentrations of eBC, eBC_{ff} and eBC_{bb}, however, it should be remembered that eBC is not a pollutant covered by air quality standards. The analysis of the results showed that in the case of total eBC and the two eBC fractions, a time coverage of 100% was obtained—therefore, the requirement of data reliability was met.

The next step in the verification of the results was the assessment of the normality of the distribution of the 24-h data sets. It was related to the possibility of using the parametric Student's *t*-test, which is much more powerful compared to typical non-parametric tests such as the U-Mann Whitney test [62–64]. First, the frequency distributions of the daily averaged mass concentrations of the analyzed pollutants were prepared, both for the data from the entire measurement period as well as by the heating and non-heating season (Figure 2). The dataset distribution was evaluated using the Kolmogorov-Smirnov test ($\alpha = 0.05$)—among the tested pollutants, only O_3 daily mass concentrations showed a normal distribution. The remaining data were log-transformed. Subsequently, the seasonal variability of the mass concentrations of the measured substances was analyzed (Student's *t*-test, $\alpha = 0.05$). The interrelationships between eBC concentration and meteorological parameters as well as the mass concentration of selected gaseous pollutants measured at the sampling site were examined by Pearson correlation analysis ($\alpha = 0.05$), separately for the data set from the heating and non-heating season. All statistical analyses were performed using the Stat Soft software package Statistica 12.0.

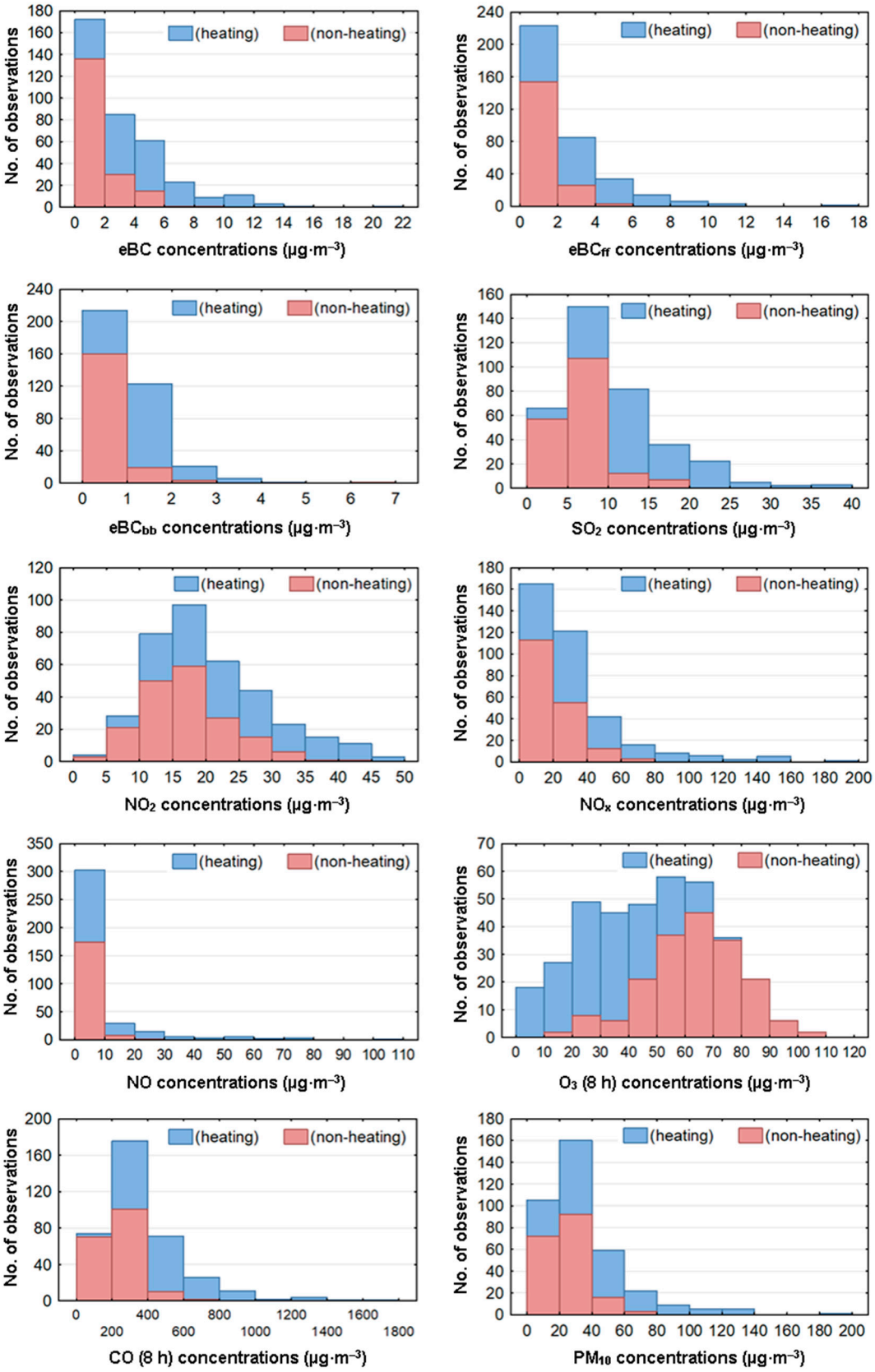

Figure 2. The frequency distribution of daily averaged concentrations of analyzed pollutants (period: 1 April 2019–30 March 2020).

3. Results and Discussion

3.1. Diurnal Variations of eBC Concentrations

During the annual measurement period, 1-h averages of eBC, eBC_{ff}, and eBC_{bb} concentrations were in the range 0.01–65.99, 0.00–64.14, and 0.00–17.20 $\mu g \cdot m^{-3}$, respectively (Figure 3). Similar to the city station in Wuhan [65], the minimum concentrations of eBC, eBC_{ff} and eBC_{bb} were recorded in the non-heating season, while the maximum concentrations were in the heating one. In Zabrze, a much larger spread of the results around the mean value was observed in the heating season, which may indicate a significant contribution of local sources to air pollution by black carbon [66]. To get more insight into the daily fluctuations of the concentrations of the 3 components under consideration, hourly eBC, eBC_{ff}, and eBC_{bb} concentrations in monthly courses were presented (Figure 4). It was found that—besides the seasonal variations—eBC, eBC_{ff}, and eBC_{bb} concentrations also exhibit pronounced diurnal variability, which could be associated with the combined effect of variations in the production of eBC, meteorology, and the associated boundary layer dynamics [23]. Distinct daily fluctuations in eBC concentrations were also identified at two research stations in Gucheng and Shangri-La, China [67].

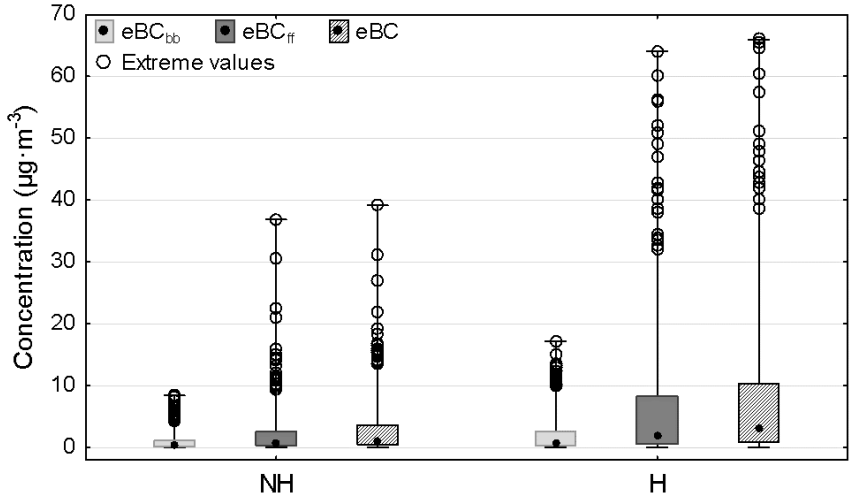

Figure 3. Box and Whisker plots for hourly averaged concentrations of eBC, eBC_{ff}, and eBC_{bb}, separately for the non-heating (NH) and heating (H) season. (The dot represents the median value; the box is marked by the 10th and 90th percentiles, and the whiskers—by the minimum and maximum values).

The lowest levels of eBC were recorded in the afternoon and from May to October and they did not exceed 1 $\mu g \cdot m^{-3}$. The minimum values of BC mass concentrations occurred at around 14:00–17:00 in July. In the case of two fractions—eBC_{ff} and eBC_{bb}—relatively low mass concentrations in the non-heating season were also recorded before noon (eBC_{ff}, 10:00–17:00) from morning to evening (eBC_{bb}, 8:00–18:00). Such low eBC concentrations at this time of day may have been caused by the diurnal variability of the meteorological conditions [22].

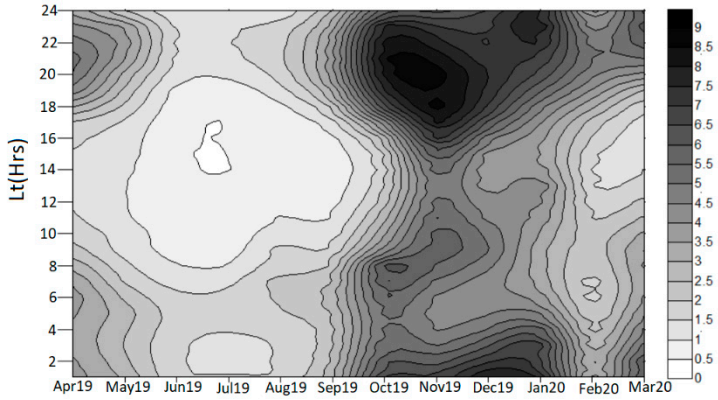

(**a**)

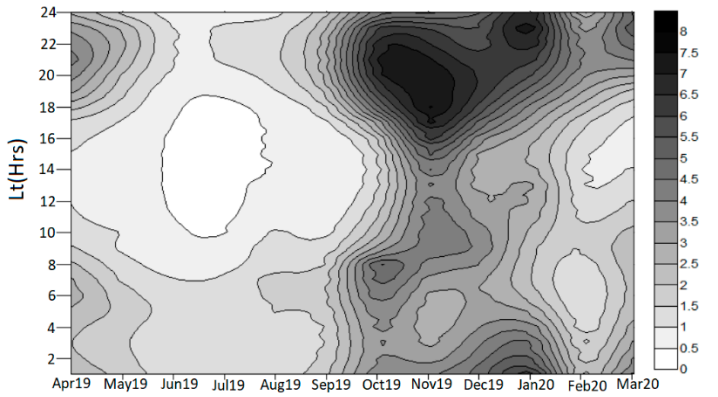

(**b**)

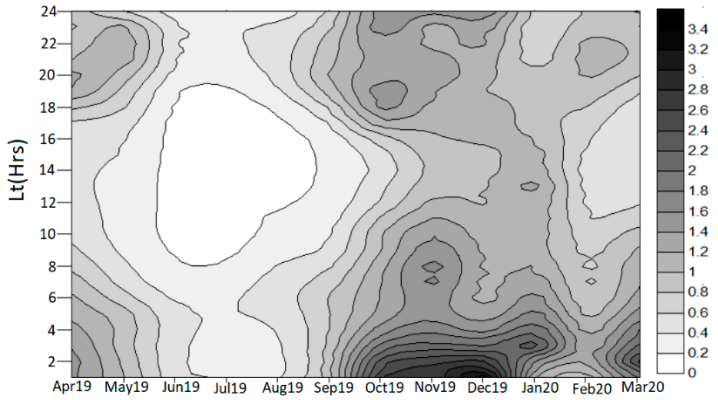

(**c**)

Figure 4. Monthly-hourly variations of surface: eBC (**a**), eBC_{ff} (**b**), and eBC_{bb} (**c**) mass concentrations ($\mu g \cdot m^{-3}$). (Monthly-hourly variations of surface: eBC, eBC_{ff} and eBC_{bb} were made using the SURFER 8 software).

With the start of the heating season (from September 2019 to March 2020), the concentrations of eBC and its components begin to increase systematically. At this time of the year, there are two distinct periods of maximum eBC mass concentrations—the first in the morning (7:00–9:00) and the second, more intense, in the evening and night hours (17:00–23:00). The obtained results are consistent with the results of numerous literature studies, which indicate that the reason for this diurnal maxima was related to the atmospheric stability and the increase of human activities [1,21,68,69]. The morning peak corresponds with increases of morning traffic during work commutes. It could be also associated with

the fumigation effect in the boundary layer, which brings aerosols from the nocturnal residual layer shortly after the sunrise [1]. The increasing eBC concentrations towards the evening might be influenced by both the residential cooking and heating, as well as the homecoming traffic overlapping gradually [21,32]. It should be noted that in the non-heating season, especially in the summer months (June–August), the two mentioned maxima are very poorly visible. The reason may be a significant decrease in the intensity of eBC emissions from anthropogenic sources and the presence of conditions favoring the dispersion of pollutants, including higher air temperature and wind speed, responsible for the increase in the height of the mixing layer, and more frequent and intense precipitation contributing to a more efficient washing of BC associated with atmospheric PM [26,69].

As depicted in Figure 4, isolines of maximum eBC and eBC_{ff} mass concentrations are very similar. A different situation was observed in the eBC_{bb} mass concentration distribution scheme. Whereas the eBC and eBC_{ff} diurnal profile was generally bimodal, the diurnal profile of eBC_{bb} showed an increase towards the night hours (1:00–4:00), which was also observed in Tiwari [22] and Helin [32]. Very low mass concentrations of eBC_{bb} in the non-heating season and the lack of a morning maximum should not be questionable due to the high impact of communication sources of emissions in these periods [70,71]. Generally, evening and night hours are conducive to intensifying BC concentrations from the combustion of fossil fuels (eBC_{ff}). However, in addition to coal burning, wood, shrubs and various waste plant materials are also burnt in households during cold winter months [1,32]. This may explain the observed monthly-hourly variation of eBC_{bb} mass concentrations and indicate the high impact of municipal emission sources—which are largely difficult to control—on air quality in Zabrze.

3.2. Daily Variations of eBC—A Seasonal Behavior

Day-to-day variability of eBC_{ff} and eBC_{bb} mass concentrations, along with their average seasonal contribution in total eBC, is displayed in Figure 5. In the entire measurement period, eBC, eBC_{ff}, and eBC_{bb} mass concentrations were in the range 0.39–20.48 $\mu g \cdot m^{-3}$, 0.32–16.08 $\mu g \cdot m^{-3}$, and 0.06–4.40 $\mu g \cdot m^{-3}$, respectively (Table 2). The average annual eBC concentration was 3.22 $\pm$ 2.80 $\mu g \cdot m^{-3}$, similar to the value obtained for the urban background station in Barcelona, Spain (3 $\mu g \cdot m^{-3}$) [72] and urban station in Ostrava, Czech Republic (3.48 $\mu g \cdot m^{-3}$) [73]. Lower concentrations of eBC were reported in some European locations—e.g., Istanbul, Turkey (2.76 $\mu g\ m^{-3}$; 1 May 2019–1 February 2020) [74] and three urban stations in the UK (2015): Birmingham (1.1 $\mu g \cdot m^{-3}$), Glasgow (0.9 $\mu g \cdot m^{-3}$), and North Kensington (1.0 $\mu g \cdot m^{-3}$) [63]. Higher than the values obtained in Zabrze, concentrations of eBC are recorded at many measurement sites in Asia, e.g., at the urban background station in Pulchowk Campus, Nepal (8.60 $\mu g \cdot m^{-3}$, May 2009–April 2010) [75] and in Xi'an, China (above 10 $\mu g \cdot m^{-3}$, 2006–2015) [65].

There were clear seasonal variations of eBC, eBC_{ff}, and eBC_{bb} concentration levels (Table 2, Figure 5). They were strongly elevated during the heating season, which was also noted in other studies conducted in sites under the influence of "residential heating sources" [32]. The observed seasonal fluctuations may also be related to the prevailing meteorological situation. In the winter, a set of unfavorable weather conditions (such as low air temperatures, low wind speeds, and frequent occurrence of the inversion layer) significantly impedes the dispersion and removal of air pollutants [41,44,76–78]. Similar seasonal variability was also observed for the remaining gaseous and particulate pollutants measured at measurement sites in Zabrze (Table 2). An exception may be ozone, which is a typical secondary air pollutant, and its maximum concentrations occur in spring-summer months.

Table 2. Descriptive statistics of the series of eBC, eBC_{ff}, eBC_{bb} and other pollutants concentration measurements—24-h concentrations over the entire period, divided into non-heating and heating seasons.

Substance	Limit Value	Concentration [μg·m^{-3}]						H/NH Ratio [e]
		Entire		Non-Heating		Heating		
		Ave ± SD	Range	Ave ± SD	Range	Ave ± SD	Range	
eBC	-	3.22 ± 2.81	0.39–20.48	1.75 ± 1.26	0.39–8.02	4.70 ± 3.13	0.88–20.48	2.69
eBC_{ff}	-	2.33 ± 2.16	0.32–16.08	1.28 ± 0.93	0.32–5.92	3.39 ± 2.51	0.53–16.08	2.65
eBC_{bb}	-	0.93 ± 0.76	0.06–6.33	0.55 ± 0.61	0.06–6.33	1.32 ± 0.69	0.27–4.40	2.41
SO_2	125 [a]	10.31 ± 6.34	1.97–38.50	6.60 ± 2.95	1.97–17.03	14.02 ± 6.65	1.99–38.50	2.12
NO_2	200 [b] 40 [c]	20.30 ± 8.95	2.88–47.04	16.95 ± 6.66	2.88–41.67	23.65 ± 9.69	4.54–47.04	1.40
NO_x	-	31.52 ± 26.95	3.79–197.38	21.50 ± 11.03	3.79–65.96	41.55 ± 33.65	5.75–197.38	1.93
NO	-	7.32 ± 13.03	0.04–103.00	2.97 ± 3.42	0.04–21.42	11.68 ± 17.05	0.42–103.00	3.93
O_3	120 [d]	48.45 ± 22.66	3.42–109.54	63.55 ± 16.93	18.71–109.54	33.35 ± 17.00	3.42–76.79	0.52
CO	10,000 [d]	364.81 ± 228.28	129.17–1778.13	240.94 ± 93.20	129.17–706.75	488.74 ± 254.84	180.33–1778.13	2.03
PM_{10}	50 [a] 40 [c]	34.49 ± 24.00 (episodes [f]: 68 days)	6.67–195.04	24.71 ± 11.49 (episodes [f]: 9 days)	6.67–75.67	44.28 ± 28.83 (episodes [f]: 59 days)	9.67–195.04	1.79

Designations: Limit value—for the protection of human health (according to Directive 2008/50/EC); Ave ± SD—average ± standard deviation; range—minimum–maximum. [a] Averaging period: day; [b] averaging period: 1 h; [c] averaging period: calendar year; [d] averaging period: 8 h; [e] H/NH ratio—ratio of the average concentration of a given substance during the heating (H) and non-heating (NH) period; the bold and underlined type indicates statistically significant differences between daily averaged concentrations of a given substance recorded during the compared periods (the Student's *t*-test, $\alpha = 0.05$); [f] the episode was considered as a case of exceeding the limit value for the average daily concentration of PM_{10}.

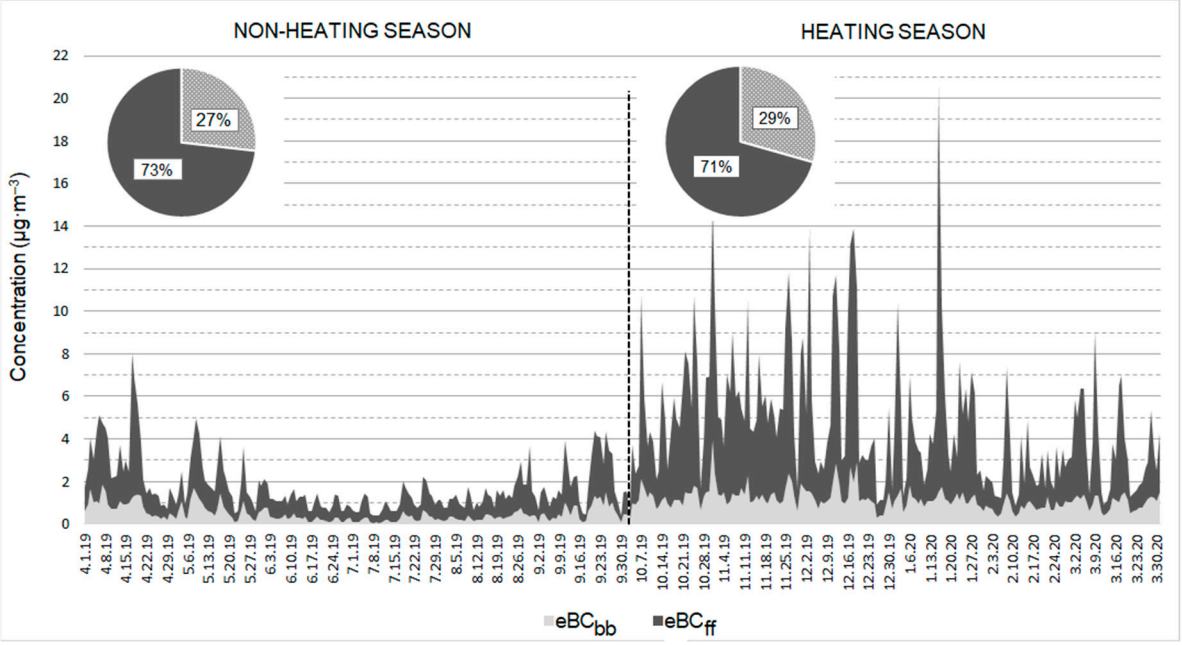

Figure 5. The daily BC_{ff} and BC_{bb} concentration courses (μg·m^{-3}) and their average share in the total BC (%) recorded for the heating and non-heating season.

Regardless of the season, the obtained results indicate much higher concentrations of eBC_{ff} compared to eBC_{bb} (Figure 5). Moreover, in the entire measurement periods, there were as many as 22 episodes (16—non-heating period, 6—heating period) during which eBC_{ff} accounted for 100% of the total eBC_{ff} content; for eBC_{bb}, there was only one such episode in the non-heating season. Obtained results are in line with the results of numerous literature studies—long-term measurement trends confirm the dominant role of fossil fuel combustion in urban air pollution by carbonaceous compounds [64,79,80]. The share of biomass burning will be visible mainly in areas of dense rural development [32,81]. In the non-heating season, the concentration of eBC_{ff} was 1.28 μg·m^{-3} and eBC_{bb} 0.55 μg·m^{-3}, which corresponded to 73% and 27% of the total BC content, respectively. In the heating season, the concentrations of eBC_{ff} and eBC_{bb} were more than twice as high, with average

values of 3.39 μg·m^{-3} and 1.32 μg·m^{-3}, respectively. Despite this, the percentage of both fractions in the total BC content was similar (average: 71% and 29%, respectively). The slight increase in the share of eBC_{ff} in total eBC recorded in the non-heating season may result from the increased importance of the combustion of liquid fossil fuels in motor vehicles at this time of the year.

3.3. eBC Concentrations vs. Gaseous Pollution and PM_{10}

The results of the parametric correlation analysis between the average daily concentrations of eBC, eBC_{ff}, and eBC_{bb} and the concentrations of gaseous and particulate pollutants (RIEP data) are presented in Table 3. For the remaining data included in Table 2, it should be noted that the concentrations of the measured gaseous pollutants did not exceed the normative levels regulated by the provisions of European law [47]. The poor air quality in the analyzed area resulted from the relatively high concentrations of PM_{10}, as evidenced by the high number of days with exceedance of the limit value for the average daily concentration of PM_{10}—68 days in the entire measurement period, almost twice as much as the accepted 35 days [47]. Much worse living conditions of the inhabitants of the urban area of Zabrze, related to the exposure to PM_{10}, occurred in the heating season, when the average concentrations of PM_{10} were almost twice as high. This is consistent with numerous literature reports on the relatively regular occurrence of very unfavorable air quality at the beginning and the end of the year [81–83].

The correlation analysis was performed for the annual measurement period—in order to capture some general relationships—as well as separately for the dataset from the heating and non-heating season—due to the emission specificity of both measurement periods. Considering the entire measurement period, all correlations between eBC, eBC_{ff}, eBC_{bb}, and other substances were statistically significant. High and very high correlations were noted especially in the heating season, with positive values of the correlation coefficients. This suggests common sources of origin of the black carbon and measured gaseous and particulate pollutants in the urban area of Zabrze—such as road transport and/or the burning of fossil fuels and biomass. The only exception is ozone—a typical secondary air pollutant with high levels during the non-heating season (see Figure 2)—with which concentrations of eBC and eBC fractions correlated negatively. In the non-heating season, a slight weakening of the relationship between concentrations of eBC and other substances was observed due to a marked decrease in the activity of local emission sources in this period, especially fuel combustion for heating purposes, and much more favorable conditions for the dispersion of pollutants [71,76,84].

Table 3. Results of the Pearson correlation analysis (α = 0.05) between concentrations of eBC, eBC_{ff}, eBC_{bb}, and concentrations of gaseous and particulate pollutants.

Specification	Year			Non-Heating			Heating		
	eBC	**eBC_{ff}**	**eBC_{bb}**	**eBC**	**eBC_{ff}**	**eBC_{bb}**	**eBC**	**eBC_{ff}**	**eBC_{bb}**
SO_2	*0.76*	*0.75*	*0.75*	*0.55*	*0.58*	*0.60*	*0.66*	*0.65*	*0.64*
NO_2	*0.78*	*0.80*	*0.67*	*0.67*	*0.71*	*0.57*	*0.83*	*0.84*	*0.75*
NO_x	*0.84*	*0.86*	*0.71*	*0.72*	*0.75*	*0.60*	*0.90*	*0.90*	*0.83*
NO	*0.82*	*0.84*	*0.70*	*0.65*	*0.68*	*0.52*	*0.89*	*0.89*	*0.83*
O_3	*−0.69*	*−0.68*	*−0.64*	*−0.27*	*−0.26*	*−0.27*	*−0.67*	*−0.68*	*−0.57*
CO	*0.87*	*0.86*	*0.84*	*0.80*	*0.79*	*0.83*	*0.80*	*0.80*	*0.73*
PM_{10}	*0.83*	*0.86*	*0.75*	*0.67*	*0.70*	*0.66*	*0.90*	*0.90*	*0.85*

Italic type indicates that the correlation is statistically significant (α = 0.05).

Taking into account the data from the entire measurement period, the strongest positive correlation was recorded for eBC, eBC_{ff}, and eBC_{bb} vs. CO (r = 0.84–0.87). A very high positive correlation between eBC and eBC fractions and CO was maintained both in the heating and non-heating season, which is typical for traffic-influenced urban monitoring sites [43,67]. However, in the non-heating season, slightly higher values of correlation coefficients were recorded for the relation eBC_{bb} vs. CO (r = 0.83). This can be explained by the influence of incomplete biomass combustion processes in municipal

sources, including open-burning activities, which can also be important sources of carbon monoxide emissions in the air at this time of the year [85].

In the heating season, the highest values of the correlation coefficient were noted for the relation eBC, eBC_{ff}, and eBC_{bb} vs. NO_x and PM_{10} (r = 0.83–0.90). This is due to an additional source of NO_x and PM_{10} emissions in this period, i.e., the combustion of fossil fuels and biomass in individual heating sector and transport, the impact of which, however, is rather constant throughout the calendar year [29,64]. In general, the concentrations of eBC_{ff} correlated more strongly with the concentrations of gaseous nitrogen oxides in comparison to eBC_{bb}, mainly due to the common source of origin, which is road transport [71,79,82]. Stronger correlations of eBC_{ff}/NO_x and eBC_{ff}/PM_{10} compared to eBC_{bb}/NO_x and eBC_{bb}/PM_{10} have been observed mainly in the non-heating season, when the influence of traffic sources is often more pronounced [76,86,87]. Nevertheless, the correlations noted between eBC_{bb} and the mentioned gaseous substances and PM_{10} were also high and statistically significant, especially during the heating season. Such a phenomenon is quite common during the heating season because one of the main sources of NO_2 emissions is the burning of municipal solid waste or the burning of biomass to generate energy [88,89].

Two measured eBC fractions also showed a very high correlation with SO_2, with comparable values of the correlation coefficients for eBC_{ff} and eBC_{bb} (r = 0.75, entire measurement period). Sulfur dioxide is a pollutant generated by domestic and industrial combustion of various fuels, including coal and biomass [90]. A relatively greater importance of this group of emission sources was recorded in the heating season, which is supported by slightly higher values of correlation coefficients between eBC, eBC_{ff}, eBC_{bb} and SO_2. As indicated in numerous scientific publications, low air quality, both in urban and rural areas, will correspond to emissions from municipal sources, the intensity of which increases significantly during the heating season [90–92].

3.4. eBC Concentrations vs. Meteorological Parameters

The presented fluctuations in the concentrations of eBC, eBC_{ff}, and eBC_{bb} may depend, on the one hand, directly on the emission sources, and, on the other hand, on the current meteorological conditions. Similarly to the concentrations of eBC, eBC_{ff}, and eBC_{bb}, the daily variability of such parameters as temperature, relative humidity, pressure, solar radiation, wind speed and rainfall total throughout the measurement year was presented (Figure 6). In order to estimate the influence of meteorological conditions on the distribution of eBC, eBC_{ff}, and eBC_{bb} concentrations, a correlation matrix was prepared (Table 4).

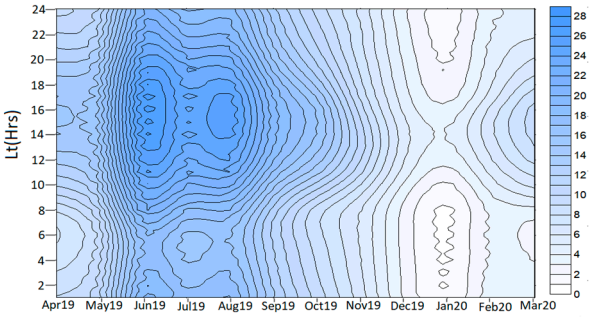

(**a**)

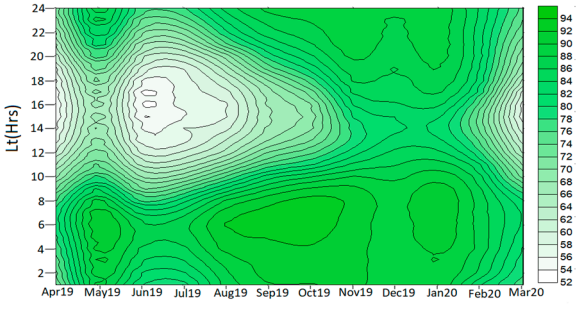

(**b**)

Figure 6. *Cont.*

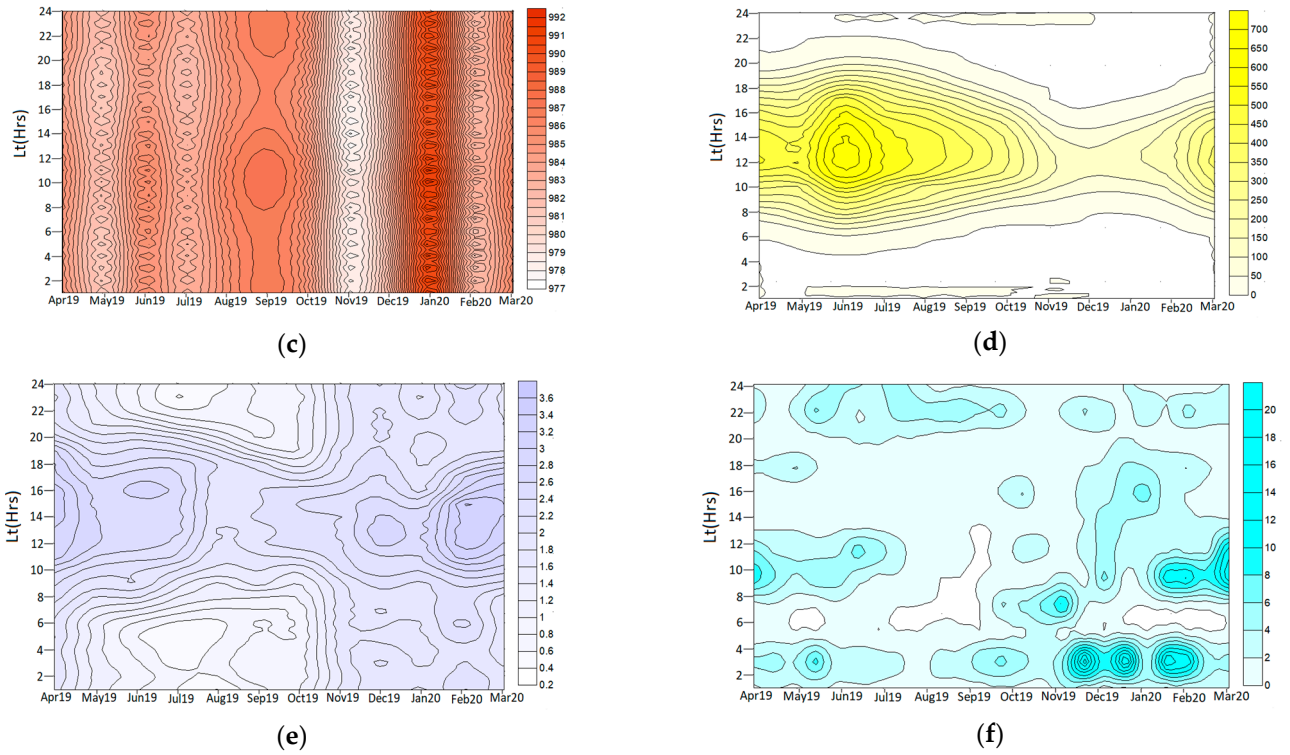

Figure 6. The monthly course of selected meteorological parameters: air temperature (°C) (**a**), relative humidity (%) (**b**), pressure (hPa) (**c**), solar radiation (W/m^2) (**d**), wind speed (m·s^{-1}) (**e**) and precipitation (l/m^2) (**f**). (Monthly-hourly variations of surface of meteorological parameters were made using the SURFER 8 software).

Table 4. The results of the Pearson correlation analysis (α = 0.05) between concentrations of eBC, eBC_{ff}, eBC_{bb}, and selected meteorological parameters.

Period	Parameter	Specification		
		eBC	**eBC_{ff}**	**eBC_{bb}**
Year	T	*−0.54*	*−0.49*	*−0.61*
	RH	*0.27*	*0.27*	*0.25*
	Bar	0.07	0.07	0.05
	SI	*−0.47*	*−0.45*	*−0.51*
	WS	*−0.14*	*−0.17*	−0.06
	Pr	*−0.23*	*−0.22*	*−0.21*
Non-heating	T	*−0.41*	*−0.31*	*−0.31*
	RH	−0.06	−0.06	−0.07
	Bar	0.10	*0.17*	*0.18*
	SI	−0.12	−0.11	−0.07
	WS	−0.11	*−0.19*	*−0.20*
	Pr	*−0.17*	*−0.16*	*−0.15*
Heating	T	0.00	0.06	0.04
	RH	0.11	*0.16*	*0.15*
	Bar	0.05	0.04	0.04
	SI	−0.02	−0.03	−0.03
	WS	*−0.54*	*−0.60*	*−0.60*
	Pr	*−0.27*	*−0.27*	*−0.24*

Italics indicate that the correlation is statistically significant (α = 0.05).

As for the concentrations of eBC, eBC_{ff}, and eBC_{bb}, all the discussed meteorological parameters show seasonal variation. The diurnal variation is noticeable in the non-heating season for humidity (Figure 6b), wind speed, and precipitation (Figure 6e,f), and in the heating season for air temperature (Figure 6a). The intensity of solar radiation varies

throughout the measurement year and was most intensively recorded during the day (Figure 6d). Air pressure (Figure 6c) was relatively stable throughout the day in both seasons, with both the maximum and the minimum occurring in the heating season. In the non-heating season, the minimum relative air humidity, relatively low air pressure, strong sunlight, and relatively strong wind were recorded, which may favor the dispersion of eBC, eBC_{ff}, and eBC_{bb} in the atmospheric air. During the heating season, air temperature and solar radiation decreased, and humidity and pressure increased. Such meteorological conditions reduce the dispersion of pollutants in the air [93], which could have led to the intensification of eBC, eBC_{ff} and eBC_{bb} concentrations.

In the entire measurement period, the strongest correlations were recorded for eBC, eBC_{ff}, and eBC_{bb}, and for all selected meteorological parameters, except for atmospheric pressure (Table 4). This mainly applies to eBC/T ($r = -0.54$), e eBC_{ff}/T ($r = -0.49$), and eBC_{bb}/T ($r = -0.61$). The influence of air temperature on air quality is a common phenomenon because the atmospheric stability decreases with the temperature increase, which favors the development of convective conditions near the ground and, as a result, leads to the diffusion of pollutants. On the other hand, low air temperature increases the activity of anthropogenic emission sources, such as burning solid fuels and biomass for heating purposes [70]. Moderate correlation was also noted in the case of solar radiation and BC ($r = -0.47$), eBC_{ff} ($r = -0.45$), and eBC_{bb} ($r = -0.51$). Similarly, in the non-heating season, the strongest correlation was noted for eBC, eBC_{ff}, eBC_{bb}, and temperature ($r = -0.41$, -0.31, and -0.31, respectively). In the case of other meteorological parameters, the observed correlations with eBC, eBC_{ff}, and eBC_{bb} were relatively low, and for humidity and solar radiation they were not statistically significant. A different situation was noted in the heating season, during which no significant correlations between eBC, eBC_{ff}, and eBC_{bb}, and air temperature were noticed. On the other hand, the impact of wind speed increased as the observed correlations with eBC, eBC_{ff}, and eBC_{bb} were the strongest in this case ($r = -0.54$, -0.60, and -0.60 respectively). The analysis of the relationship between the concentration of eBC and meteorological parameters indicates the compliance with other studies at city stations (Delhi, India and Ostrava, Czech Republic), in which for the measurement year eBC was the strongest negatively correlated with air temperature [22,69]. The negative correlation of pollutant concentrations with air temperature, wind speed, and precipitation is a common phenomenon and has been noted, among others, in for $PM_{2.5}$ at municipal stations in China [94], Japan [95], and the United States [96]. Moreover, it was noticed that in the city station in the Czech Republic, the correlations are also usually higher on the annual average than in the case of the average for the non-heating and heating season. The lack of statistically significant relationships with the temperature of the analyzed substances in the heating season may indicate that other factors, such as long-range transport events, episodes of regional recirculation, or complex photochemical reactions, may have a greater influence on high concentrations of these substances [97,98]. A similar situation was also observed in other studies [99] and it may indicate the dominant influence of local emission sources. Due to the clear variability of the relationship between eBC, eBC_{ff}, and eBC_{bb} with meteorological parameters, the variability of the share of these substances in relation to the type of circulation in the heating season was checked.

3.5. BC Concentrations vs. Air Circulation

The analysis of the influence of atmospheric circulation types and the type of air masses on the distribution of eBC, eBC_{ff}, and eBC_{bb} concentrations (Figure 7) showed seasonal differences in terms of the dominant sectors. In both measurement seasons, differences were observed in the distribution of eBC, eBC_{ff}, and eBC_{bb} concentrations for individual types of circulation. Moreover, the distributions of the components eBC_{ff} and eBC_{bb} for individual types of circulation were analogous to the distribution of eBC. In the non-heating season (Figure 7a), both anticyclonal and cyclonal circulations played an important role in shaping the level of eBC, eBC_{ff}, and eBC_{bb}. During anticyclonal circulations, the greatest importance in shaping elevated levels of BC (>2 $\mu g \cdot m^{-3}$), eBC_{ff} (>1 μg $\mu g \cdot m^{-3}$) and eBC_{bb}

(>0.5 μg·m^{-3}) was the inflow of air masses from the eastern sector (Ea), Northeast (NEa), and South (Sa). In the case of cyclones, these were inflows from the south-eastern (SEc), southern (Sc), and eastern (Ec) sectors and unclassified situations (x).

The maximum concentration of eBC, eBC$_{ff}$, and eBC$_{bb}$ (9.37, 7.06 and 2.31 μg·m^{-3}, respectively) occurred in the heating season during the anticyclonal circulation and was related to the Ca situation (Figure 7b). In the heating season, the anticyclonal circulation of the Sa, SWa, and Wa types also had a significant influence on the high concentrations of eBC (~6 μg·m^{-3}), eBC$_{ff}$ (~4 μg·m^{-3}), and eBC$_{bb}$ (~1 μg·m^{-3}). The effect of anticyclone circulation types Sa, SWa, and Wa on the presence of high concentrations of air pollutants (PM_{10}) was also observed in Pilguj et al. (2018) [100]. High concentrations of air pollutants during anticyclonal circulation are a common phenomenon due to the fact that they are associated with unfavorable meteorological conditions (the state of equilibrium in the lower boundary layer of the atmosphere), the occurrence of which limits the dispersion of pollutants [101]. Pollution intensification, e.g., PM_{10} in winter during circulation related to the high-pressure center what was observed, among others in Leśniok [102] Pietras [103] and Pilguj [100].

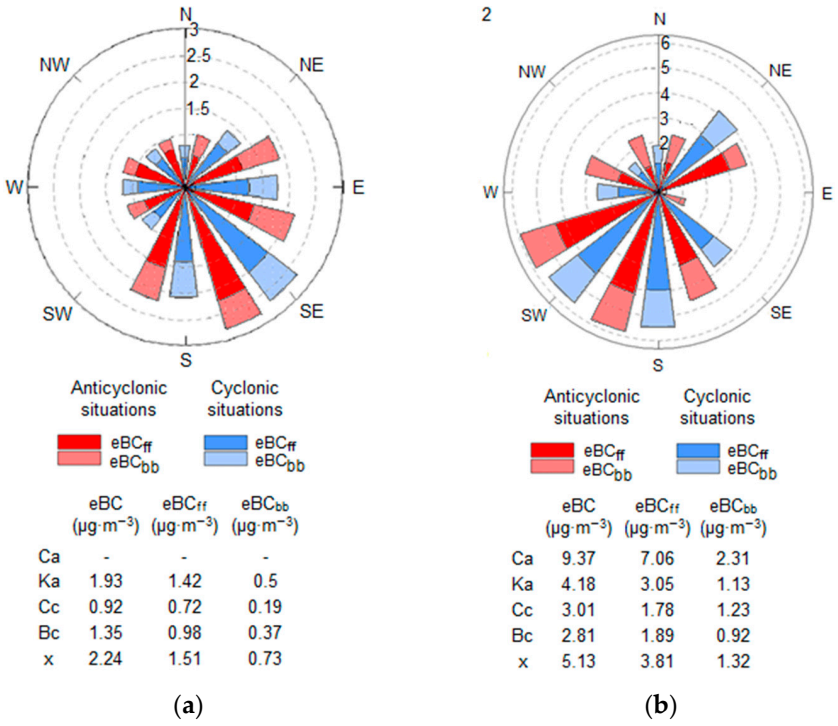

Figure 7. The average eBC, eBC$_{ff}$, and eBC$_{bb}$ (μg·m^{-3}) concentration values corresponding to particular types of circulation in the non-heating (**a**) and heating (**b**) period.

Regardless of the nature of the circulation, the highest concentrations of eBC, eBC$_{ff}$, and eBC$_{bb}$ occurred during advection of air masses from the southern sector. In the group of cyclonal types, increased concentrations of eBC, eBC$_{ff}$, and eBC$_{bb}$ were characteristic of advection from the southern (Sc) and south-western (SWc) sectors. The effect of unclassified synoptic situations on elevated concentrations of eBC, eBC$_{ff}$, and eBC$_{bb}$ was also observed (x: 5.13, 3.81 and 1.32 μg·m^{-3}, respectively).

Based on the conducted analyzes, it was shown that the circulation conditions influence the distribution of high concentrations of BC, BC$_{ff}$, and BC$_{bb}$ in Zabrze. Relatively low concentrations occurred during anticyclonal and cyclonal circulations (including unclassified synoptic situations) in the non-heating season. In addition, increased concentrations of the substances in question were associated with advection from the south (SEc, Sc), north (NEa), and east (Ea). During the heating season, the types of anticyclonal circulation were

much more often accompanied by high concentrations of eBC, eBC_{ff}, and eBC_{bb} than the cyclonal types, and their maximum concentrations occurred when the high-pressure center was over Poland (Ca). In addition, high values of eBC, eBC_{ff}, and eBC_{bb} concentrations, regardless of the circulation type, occurred most frequently during the advection of air masses from the south. It was noticed that both during the heating season and outside the heating season, increased concentrations of BC and its components occurred in the case of the influx of air masses from the east, which may indicate a significant share of road traffic in shaping the level of the measured substances. In the heating season, the intensification of BC and its components was associated with the advection of air masses from the NE, SW, S, and SE sectors, i.e., from areas characterized by residential buildings, houses and allotment areas. Such distribution of BC and its components indicates the combustion of solid fuels for heating purposes as the dominant source of emissions of the pollutants in question. In addition, the heating season is associated with the illegal burning of biomass in allotment gardens, which could also significantly increase the concentration of BC, BC_{ff}, and BC_{bb}. In the non-heating period, in addition to advection of the masses from the eastern sector, the south-eastern sector was of great importance in shaping the level of the substances in question, which indicates industry as the main source of BC, BC_{ff}, and BC_{bb}. In this case, the impact of emissions of the substances in question from allotments (NE sector) was also noticed, which may result from the increased use of common food preparation equipment, such as garden grills.

4. Conclusions

The annual eBC measurement campaign (between 1 April 2019 and 1 October 2020) concerned the urban background station located in the city center of Zabrze. The seasonal variability of BC mass concentrations was examined as well as the share of emissions from fossil fuel combustion (eBC_{ff}) and biomass (eBC_{bb}) in the total BC content for the heating (1 October 2019–31 March 2020) and non-heating season (1 April 2019–30 September 2019). It was found that the annual mean eBC concentrations (3.22 ± 2.80 $\mu g \cdot m^{-3}$) in Zabrze were generally comparable to several urban stations in Europe and lower than for urban stations in Asia and the United States. The poor air quality in the analyzed area resulted from relatively high concentrations of PM_{10}, especially the high number of days with exceedance of the limit value for the average daily concentration of PM_{10}.

It was noticed that both in the non-heating and heating season, the share of eBC_{ff} in total eBC (average: 73 and 71%, respectively) was significantly higher compared to eBC_{bb} (average: 27 and 29%, respectively). This indicated the dominant influence of fossil fuel combustion processes—both solid (households) and liquid (road transport)—on air pollution by eBC in the urban area of Zabrze. In the heating season, the concentration of the discussed eBC fractions was much higher than in the non-heating season; moreover, the diurnal fluctuations of eBC_{bb} and eBC_{ff} concentrations were definitely more pronounced. Hourly eBC concentrations follow a diurnal cycle that has been seen in other literature data, with two distinct periods of maximum eBC_{ff} concentrations—the first in the morning (7:00–9:00) and the second in the evening and night hours (17:00–23:00)—which occurrence was primarily associated with an increase in the intensity of human activities. On the contrary, the highest concentrations of eBC_{bb} were recorded only during the night hours, which may indicate a large impact of the combustion processes of wood, shrubs and various waste plant materials in households during cold winter months.

The impact of fossil fuel and wood biomass burning emissions on the measured eBC concentrations was supported by the Pearson correlation analysis between concentrations of eBC, eBC_{ff}, eBC_{bb}, and gaseous and particulate pollutants. High correlation coefficients—with a maximum for the relationships: eBC, eBC_{ff}, eBC_{bb} vs. CO and eBC, eBC_{ff} vs. NO_x—were recorded especially during the heating season, when the share of local emission sources is intense and the conditions of dispersion of pollutants are unfavorable.

The significant negative correlation between the concentrations of the eBC component and air temperature, wind speed, and the sum of precipitation indicates a significant influ-

ence of meteorological parameters in the non-heating season. On the other hand, in the heating season, a significant weakening of the relationship with temperature was observed, for eBC, eBC_{ff}, and eBC_{bb}, which may indicate a dominant influence of local emission sources, perhaps as well as other factors, such as long-range transport events, regional recirculation episodes, or complex photochemical reactions. In addition, the distribution of eBC, eBC_{ff}, and eBC_{bb} concentrations depends on the occurrence of individual types of air mass circulation. In the heating season, significantly elevated concentrations of eBC, eBC_{ff}, and eBC_{bb} were more often observed in high-pressure situations, and the maximum was associated with the high-pressure center. During the heating season, increased concentrations for both types of circulation (anticyclonal and cyclonal) were associated with the advection of air masses from the southern sector.

The results of this research on high correlations with normative air pollutants indicate that in the future the AE33 Aethalometer may be an effective device for quick and direct air quality measurement, especially in urban areas where there is a high risk of intensification of anthropogenic pollution. The monitoring of air in terms of eBC measurements and its components should be especially taken into account during the heating season, when, regardless of meteorological conditions, increased concentrations of these substances persist for most of the day. In addition, the Aethalometer is a device that quickly and easily provides information about the eBC share of biomass burning.

The results obtained in this study are valuable primarily for cognitive reasons—they enable deepening the knowledge about the content of black carbon in the ambient air and determining its emission sources. This is all the more important as in Poland—where high concentrations of particulate matter are recorded compared to many European countries—there are no systematic measurements of eBC, which due to its original nature can be a direct indicator of the impact of air pollution on the environment, climate, and population health. Such measurements may also provide important information for improving decision making, e.g., city planning and relevant source emission restrictions. It is advisable to continue the conducted research in the future, in conjunction with the extension of the scope of meteorological parameters measurements, including the assessment of the height of the mixing layer.

Author Contributions: Conceptualization, methodology, formal analysis, resources, data curation, visualization, investigation, writing—original draft preparation, review and editing, project administration, N.Z.; investigation, software, validation, writing—review and editing, English correction, formal analysis, writing—original draft preparation, B.B.; writing—review & editing, project administration, supervision, funding acquisition, K.K. All authors have read and agreed to the published version of the manuscript.

Funding: This work was supported by the Institute of Environmental Engineering of the Polish Academy of Sciences basic (statutory) research project no. 1a-119/2018 (*Temporal and spatial variability of the chemical composition of atmospheric aerosols as a tool for assessing the effects of implementing air protection programs in Poland*, 2018–2020). The work was also prepared as a part of the research project H2020 No. 654109 *Aerosols, Clouds, and Trace gases Research Infrastructure* (*ACTRIS-2*).

Data Availability Statement: The data that support the findings of this study are available from the corresponding author, upon reasonable request.

Conflicts of Interest: The authors declare no conflict of interest.

References

1. Balakrishnaiah, G.; Ragjavendra Kumar, K.; Suresh Kumar Reddy, B.; Swamulu, C.; Rama Gopal, K.; Reddy, R.R.; Reddy, L.S.S.; Nazeer Ahammed, Y.; Narasimhulu, K.; KrishnaMoorthy, K.; et al. Anthropogenic impact on the temporal variations of black carbon and surface aerosol mass concentrations at a tropical semi-arid station in southeastern region of India. *J. Asia Earth Sci.* **2011**, *42*, 1297–1308. [CrossRef]
2. Bond, T.C.; Doherty, S.J.; Fahey, D.W.; Forster, P.M.; Berntsen, T.; DeAngelo, B.J.; Flanner, M.G.; Ghan, S.; Kärcher, B.; Koch, D.; et al. Bounding the role of black carbon in the climate system: A scientific assessment. *J. Geophys. Res. Atmos.* **2013**, *118*, 5380–5552. [CrossRef]

3. IPCC. *Climate Change 2014: Synthesis Report. Contribution of Working Groups I, II and III to the Fifth Assessment Report of the Intergovernmental Panel on Climate Change*; Core Writing Team; Pachauri, R.K., Meyer, L.A., Eds.; IPCC: Geneva, Switzerland, 2014; p. 151.
4. Sandrini, S.; Fuzzi, S.; Piazzalunga, A.; Prati, P.; Bonasoni, P.; Cavalli, F.; Bove, M.C.; Calvello, M.; Cappelletti, D.; Colombi, C.; et al. Spatial and seasonal variability of carbonaceous aerosol across Italy. *Atmos. Environ.* **2014**, *99*, 587–598. [CrossRef]
5. Maciejewska, K.; Juda-Rezler, K.; Reizer, M.; Klejnowski, K. Modelling of black carbon statistical distribution and return periods of extreme concentrations. *Environ. Model. Softw.* **2015**, *74*, 212–226. [CrossRef]
6. Gelencsér, A. Major Carbonaceous Particle Types and Their Sources. Available online: https://link.springer.com/chapter/10.1007/978-1-4020-2887-8_3 (accessed on 14 January 2021).
7. Błaszczak, B.; Mathews, B. Characteristics of Carbonaceous Matter in Aerosol from Selected Urban and Rural Areas of Southern Poland. *Atmosphere* **2020**, *11*, 687. [CrossRef]
8. Rechman, I.H.; Ahmed, T.; Praveen, P.S.; Kar, A.; Ramanathan, V. Black carbon emissions from biomass and fossil fuels in rural India. *Atmos. Chem. Phys.* **2011**, *11*, 7289–7299. [CrossRef]
9. Lonati, G.; Ozgen, S.; Ripamonti, G.; Signorini, S. Variability of black carbon and ultrafine particle concentration on urban bike routes in a mid-sized city in the Po Valley (northern Italy). *Atmosphere* **2017**, *8*, 40. [CrossRef]
10. Saturno, J.; Holanda, B.A.; Pöhlker, C.; Ditas, F.; Wang, Q.; Moran-Zuloaga, D.; Brito, J.; Carbone, S.; Cheng, Y.; Chi, X.; et al. Black and brown carbon over central Amazonia: Long-term aerosol measurements at the ATTO site. *Atmos. Chem. Phys.* **2018**, *18*, 12817–12843. [CrossRef]
11. Laing, J.R.; Jaffe, D.A.; Sedlacek, A.J., III. Comparison of Filter-based Absorption Measurements of Biomass Burning Aerosol and Background Aerosol at the Mt. Bachelor Observatory. *Aerosol. Air Qual. Res.* **2020**, *20*, 663–678.
12. Kirchstetter, T.W.; Novakov, T.; Hobbs, P.V. Evidence that the spectral dependence of light absorption by aerosols is affected by organic carbon. *J. Geophys. Res.* **2004**, *109*, D21208. [CrossRef]
13. Andreae, M.O.; Gelencser, A. Black carbon or brown carbon? The nature of light-absorbing carbonaceous aerosols. *Atmos. Chem. Phys.* **2006**, *6*, 3131–3148. [CrossRef]
14. Saleh, R.; Hennigan, C.J.; McMeeking, G.R.; Chuang, W.K.; Robinson, E.S.; Coe, H.; Donahue, N.M.; Robinson, A.L. Absorptivity of brown carbon in fresh and photo-chemically aged biomass-burning emissions. *Atmos. Chem. Phys.* **2013**, *13*, 7683–7693. [CrossRef]
15. European Environment Agency. Status of Black Carbon Monitoring in Ambient Air in Europe. Available online: https://www.eea.europa.eu/publications/status-of-black-carbon-monitoring (accessed on 14 January 2021).
16. IPCC. *Climate Change 2007: Synthesis Report. Contribution of Working Groups I, II and III to the Fourth Assessment Report of the Intergovernmental Panel on Climate Change*; Core Writing Team; Pachauri, R.K., Reisinger, A., Eds.; IPCC: Geneva, Switzerland, 2007; p. 104.
17. EPA. *Report to Congress on Black Carbon, Department of the Interior, Environment, and Related Agencies Appropriations Act*; EPA-450/R-12-001 March 2012; US Environmental Protection Agency: Washington, DC, USA, 2010.
18. Dutkiewicz, V.; DeJulio, A.M.; Ahmed, T.; Laing, J. Forty-seven Years of Weekly Atmospheric Black Carbon Measurements in the Finnish Artic: Decrease in Black Carbon with Declining Emissions. *J. Geophys. Res. Atmos.* **2014**, *119*, 7667–7683. [CrossRef]
19. Li, C.; Yan, F.; Kang, S.; Chen, P.; Han, X.; Hu, Z.; Zhang, G.; Hong, Y.; Gao, S.; Qu, B.; et al. Re-evaluating black carbon in the Himalayas and the Tibetan Plateau: Concentrations and deposition. *Atmos. Chem. Phys.* **2017**, *17*, 11899–11912. [CrossRef]
20. Chýlek, P.; Kou, L.; Johnson, B.; Boudala, F.; Lesins, G. Black carbon concentrations in precipitation and near surface air in and near Halifax, Nova Scotia. *Atmos. Environ.* **1999**, *33*, 2269–2277. [CrossRef]
21. Cao, J.-J.; Zhu, C.-S.; Chow, J.C.; Watson, J.G.; Han, Y.-M.; Wang, G.-H.; Shen, Z.-X.; An, Z.-S. Black carbon relationships with emissions and meteorology in Xi'an, China. *Atmos. Res.* **2009**, *94*, 194–202. [CrossRef]
22. Tiwari, S.; Srivastava, A.K.; Bisht, D.S.; Parmita, P.; Srivastava, M.K.; Attri, S.D. Diurnal and seasonal variations of black carbon and PM2.5 over New Delhi, India: Influence of meteorology. *Atmos. Res.* **2013**, *125–126*, 50–62. [CrossRef]
23. Simpson, D.; Yttri, K.E.; Klimont, Z.; Kupiainen, K.; Caseiro, A.; Gelencsér, A.; Pio, C.; Puxbaum, H.; Legrand, M. Modeling carbonaceous aerosol over Europe: Analysis of the CARBOSOL and EMEP EC/OC campaigns. *J. Geophys. Res.* **2007**, *112*, 1–26. [CrossRef]
24. Kanaya, Y.; Taketani, F.; Komazaki, Y.; Liu, X.; Kondo, Y.; Sahu, L.K.; Irie, H.; Takashima, H. Comparison of Black Carbon Mass Concentrations Observed by Multi-Angle Absorption Photometer (MAAP) and Continuous Soot-Monitoring System (COSMOS) on Fukue Island and in Tokya, Japan. *Aerosol Sci. Technol.* **2013**, *47*, 1–10. [CrossRef]
25. Bauer, S.E.; Bausch, A.; Nazarenko, L.; Tsigardis, K.; Xu, B.; Edwards, R.; Bisiaux, M.; McConnell, J. Historical and future black carbon deposition on the three ice caps: Ice core measurements and model simulations from 1850 to 2100. *J. Geophys. Res. Atmos.* **2013**, *118*, 1–14. [CrossRef]
26. Forbes, M.S.; Raison, R.J.; Skjemstad, J.O. Formation, transformation and transport of black carbon (charcoal) in terrestrial and aquatic ecosystems. *Sci. Total Environ.* **2006**, *370*, 190–206. [CrossRef]
27. Magalhaes, S.; Baumgartner, J.; Weichenthal, S. Impacts of exposure to black carbon, elemental carbon, and ultrafine particles from indoor and outdoor sources on blood pressure in adults: A review of epidemiological evidence. *Environ. Res.* **2018**, *161*, 345–353. [CrossRef] [PubMed]

28. Wichmann, H.-E.; Spix, C.; Tuch, T.; Wölke, G.; Peters, A.; Heinrich, J.; Kreyling, W.G.; Heyder, J. *Daily Mortality and Fine and Ultrafine Particles in Erfurt, Germany, Part I: Role of Particle Number and Particle Mass, Research Report*; Health Effects Institute: Boston, United States, 2000; Volume 98, pp. 5–86.
29. Arden Pope, C., III; Dockery, D.W. Health Effects of Fine Particulate Air Pollution: Lines that Connect. *J. Air Waste Manag. Assoc.* **2006**, *56*, 709–742. [CrossRef] [PubMed]
30. Torres, A.; Bond, T.C.; Lehmann, C.M.B.; Subramanian, R.; Hadley, O.L. Measuring Organic Carbon and Black Carbon in Rainwater: Evaluation of Methods. *Aerosol Sci. Technol.* **2014**, *48*, 239–250. [CrossRef]
31. Smart Freight Centre. Black Carbon Methodology for the Logistics Sector. Available online: https://ctl.mit.edu/pub/paper/black-carbon-methodology-logistics-sector (accessed on 14 January 2021).
32. Helin, A.; Niemi, J.V.; Virkkula, A.; Pirjola, L.; Teinilä, K.; Backman, J.; Aurela, M.; Saarikoski, S.; Rönkkö, T.; Asmi, E.; et al. Characteristics and source apportionment of black carbon in the Helsinki metropolitan area. Finland. *Atmos. Environ.* **2018**, *190*, 87–98. [CrossRef]
33. Klimont, Z.; Kupiainen, K.; Heyes, C.; Purohit, P.; Cofala, J.; Rafaj, P.; Borken-Kleefeld, J.; Schöpp, W. Global anthropogenic emissions of particulate matter including black carbon. *Atmos. Chem. Phys.* **2017**, *17*, 8681–8723. [CrossRef]
34. Berkowicz, R.; Hertel, O.; Larsen, S.E.; Sørensen, N.N.; Nielsen, M. *Modelling Traffic Pollution in Streets*; National Environmental Research Institute: Roskilde, Denmark, 1997.
35. Gulia, S.; Nagendra, S.M.S.; Khare, M.; Khanna, I. Urban air quality management—A review. *Atmos. Pollut. Res.* **2015**, *6*, 286–304. [CrossRef]
36. Grundstrom, M.; Tang, L.; Hallquist, M.; Nguyen, H.; Chen, D.; Pleijel, H. Influence of atmospheric circulation patterns on urban air quality during the winter. *Atmos. Pollut. Res.* **2015**, *6*, 278–285. [CrossRef]
37. Briggs, N.L.; Long, C.M. Critical review of black carbon and elemental carbon source apportionment in Europe and the United States. *Atmos. Environ.* **2016**, *144*, 409–427. [CrossRef]
38. Invernizzi, G.; Ruprecht, A.; Mazza, R.; De Marco, C.; Močnik, G.; Sioutas, C.; Westerdahl, D. Measurement of black carbon concentration as an indicator of air qualitybenefits of traffic restriction policies within the ecopass zone in Milan. Italy. *Atmos. Environ.* **2011**, *45*, 3522–3527. [CrossRef]
39. Titos, G.; Lyamani, H.; Drinovec, L.; Olmo, F.J.; Močnik, G.; Alados-Arboledas, L. Evaluation of the impact of transportation changes on air quality. *Atmos. Environ.* **2015**, *114*, 19–31. [CrossRef]
40. Ježek, I.; Blond, N.; Skupinski, G.; Močnik, G. The traffic emission-dispersion model for a Central-European city agrees with measured black carbon apportioned to traffic. *Atmosp. Environ.* **2018**, *184*, 177–190. [CrossRef]
41. Herich, H.; Hueglin, C.; Buchmann, B. A 2.5 year's source apportionment study of black carbon from wood burning and fossil fuel combustion at urban and rural sites in Switzerland. *Atmos. Meas. Tech.* **2011**, *4*, 1409–1420. [CrossRef]
42. Schleicher, N.; Cen, K.; Norra, S. Daily variations of black carbon and element concentrations of atmospheric particles in the Beijing megacity—Part 1: General temporal course and source identification. *Chemie der Erde* **2013**, *73*, 51–60. [CrossRef]
43. Crilley, L.R.; Bloss, W.J.; Yin, J.; Beddows, D.C.S.; Harrison, R.M.; Allan, J.D.; Young, D.E.; Flynn, M.; Williams, P.; Zotter, P.; et al. Sources and contributions of wood smoke during winter in London: Assessing local and regional influences. *Atmos. Chem. Phys.* **2015**, *15*, 3149–3171. [CrossRef]
44. Becerril-Valle, M.; Coz, E.; Prévôt, A.; Močnik, G.; Pandis, S.; de la Campa, A.S.; Alastuey, A.; Díaz, E.; Pérez, R.; Artíñano, B. Characterization of atmospheric black carbon and co-pollutants in urban and rural areas of Spain. *Atmos. Environ.* **2017**, *169*, 36–53. [CrossRef]
45. Healy, R.; Sofowote, U.; Su, Y.; Debosz, J.; Noble, M.; Jeong, C.-H.; Wang, J.; Hilker, N.; Evans, G.; Doerksen, G. Ambient measurements and source apportionment of fossil fuel and biomass burning black carbon in Ontario. *Atmos. Environ.* **2017**, *161*, 34–47. [CrossRef]
46. Juda-Rezler, K.; Reizer, M.; Maciejewska, K.; Błaszczak, B.; Klejnowski, K. Characterization of atmospheric PM2.5sources at a Central Europeanurban background site. *Sci. Total Environ.* **2020**, *713*, 136729. [CrossRef]
47. Commission Directive. Directive 2008/50/EC of the European Parliament and Council of 21.05.2008 on Air Quality and Cleaner Air in Europe. Available online: http://extwprlegs1.fao.org/docs/pdf/eur80016.pdf (accessed on 14 January 2021).
48. Chief Inspectorate of Environmental Protection. Air Quality Portal. Available online: http://powietrze.gios.gov.pl/pjp/current?lang=en (accessed on 20 September 2018).
49. Niedźwiedź, T. *Calendar of Atmosphere Circulation Types for Southern Poland—Computer Collection*; University of Silesia, Department of Climatology: Sosnowiec, Poland, 2017.
50. Lamb, H.H. *British Isles Weather Types and a Register of Daily Sequence of Circulation Patterns, 1861–1971*; Geophysical Memoir, 116; HMSO: London, UK, 1972; p. 85.
51. Petzold, A.; Schloesser, H.; Sheridan, P.J.; Arnott, W.P.; Ogren, J.A.; Virkkula, A. Evaluation of Multiangle Absorption Photometry for Measuring Aerosol Light Absorption. *Aerosol Sci. Technol.* **2005**, *39*, 40–51. [CrossRef]
52. Drinovec, L.; Močnik, G.; Zotter, P.; Prévôt, A.S.H.; Ruckstuhl, C.; Coz, E.; Rupakheti, M.; Sciare, J.; Müller, T.; Wiedensohler, A.; et al. The "dual-spot" Aethalometer: An improved measurement of aerosol black carbon with real-time loading compensation. *Atmos. Meas. Tech.* **2015**, *8*, 1965–1979. [CrossRef]
53. Sedlacek, A.J. *AethalometerTM Instrumental Handbook*; DOE/SC-ARM-TR-156; ARM Climate Research Facility: Billings, MT, USA, 2016.

54. Magee Scientific. Magee Scientific Aerosol d.o.o, Aethalometer Model AE33 User's Manual. Available online: https://www.benchmarkmonitoring.com.au/sites/default/files/documents/AE33_UsersManual_Rev154.pdf (accessed on 14 January 2021).
55. Liu, D.; He, C.; Schwarz, J.P.; Wang, X. Lifecycle of light-absorbing carbonaceous aerosols in the atmosphere. *Clim. Atmos. Sci.* **2020**, *3*, 40. [CrossRef]
56. Hoffer, A.; Tóth, A.; Pósfai, M.; Chung, C.E.; Gelencsér, A. Brown carbon absorption in the red and near infrared spectral region. *Atmos. Chem. Phys. Discuss.* **2016**. [CrossRef]
57. Sandradewi, J.; Prévôt, A.S.H.; Alfarra, M.R.; Szidat, S.; Wehrli, M.N.; Ruff, M.; Weimer, S.; Lanz, V.A.; Weingartner, E.; Perron, N.; et al. Comparison of several wood smoke markers and source apportionment methods for wood burning particulate mass. *Atmos. Chem. Phys.* **2008**, *8*, 8091–8118. [CrossRef]
58. Belis, C.A.; Larsen, B.R.; Amati, F.; Haddad, I.E.; Favez, O.; Harrison, R.M.; Hopke, P.K.; Nava, S.; Paatero, P.; Prévôt, A.; et al. European Guide on Air Pollution Source Apportionment with Receptor Models. Available online: https://ec.europa.eu/jrc/en/publication/reference-reports/european-guide-air-pollution-source-apportionment-receptor-models (accessed on 14 January 2021).
59. Zotter, P.; Herich, H.; Gysel, M.; El-Haddad, I.; Zgang, Y.; Močnik, G.; Hüglin, C.; Baltensperger, U.; Szidat, S.; Prévôt, A.S.H. Evaluation of the absorption Ångström exponents for traffic and wood burning in the Aethalometer-based source apportionment using radiocarbon measurements of ambient aerosol. *Atmos. Chem. Phys.* **2017**, *17*, 4229–4249. [CrossRef]
60. Harrison, R.M.; Beddows, D.C.S.; Hu, L.; Yin, J. Comparison of methods for evaluation of wood smoke and estimation of UK ambient concentrations. *Atmos. Chem. Phys. Discuss.* **2012**, *12*, 6805–6838. [CrossRef]
61. Petzold, A.; Baltensperger, U.; Holzer-Popp, T.; Pappalardo, G. Recommendations for reporting "black carbon" measurements. *Atmos. Chem. Phys.* **2013**, *13*, 8365–8379. [CrossRef]
62. Innocente, E.; Squizzato, S.; Visin, F.; Facca, C.; Rampazzo, G.; Bertolini, V.; Gandolfi, I.; Franzetti, A.; Ambrosini, R.; Bestetti, G. Influence of seasonality, air mass origin and particulate matter chemical composition on airborne bacterial community structure in the Po Valley, Italy. *Sci. Total Environ.* **2017**, *593–594*, 677–687. [CrossRef] [PubMed]
63. Srivastava, D.; Favez, O.; Bonnaire, N.; Lucarelli, F.; Haeffelin, M.; Perraudin, E.; Gros, V.; Villenave, E.; Albinet, A. Speciation of organic fractions does matter for aerosol source apportionment. Part 2: Intensive short-term campaign in the Paris area (France). *Sci. Total Environ.* **2018**, *634*, 267–278. [CrossRef] [PubMed]
64. Bandowe, B.A.M.; Nkansah, M.A.; Leimer, S.; Fischer, D.; Lammel, G.; Han, Y. Chemical (C, N, S, black carbon) and stable isotope composition of street dusts from a major West African metropolis: Implications for source apportionment and exposure. *Sci. Total Environ.* **2019**, *655*, 1468–1478. [CrossRef]
65. Gong, W.; Zhang, T.; Zhu, Z.; Ma, Y. Characteristics of $PM_{1.0}$, $PM_{2.5}$, and PM_{10}, and Their Relation to Black Carbon in Wuhan, Central China. *Atmosphere* **2015**, *6*, 1377–1387. [CrossRef]
66. Jones, A.M.; Harrison, R.M. Interpretation of particulate elemental andorganic carbon concentrations at rural, urban andkerbside sites. *Atmos. Environ.* **2005**, *39*, 7114–7126. [CrossRef]
67. Guo, B.; Wang, Y.; Zhang, X.; Che, H.; Ming, J.; Yi, Z. Long-Term Variation of Black Carbon Aerosol in China Based on Revised Aethalometer Monitoring Data. *Atmosphere* **2020**, *11*, 684. [CrossRef]
68. Rattigan, O.V.; Civerolo, K.; Doraiswamy, P.; Felton, H.D.; Hopke, P.K. Long term Black Carbon Measurements at Two Urban Locations in New York. *AAQR.* **2013**, *13*, 1181–1196. [CrossRef]
69. Tian, J.; Fang, C.; Qiu, J.; Wang, J. Analysis of Pollution Characteristics and Influencing Factors of Main Pollutants in the Atmosphere of Shenyang City. *Atmosphere* **2020**, *11*, 766. [CrossRef]
70. Järvi, L.; Junninen, H.; Karppinen, A.; Hillamo, R.; Virkkula, A.; Mäkelä, T.; Pakkanen, T.; Kulmala, M. Temporal variations in black carbon concentrations with different time scales in Helsinki during 1996–2005. *Atmos. Chem. Phys.* **2008**, *8*, 1017–1027. [CrossRef]
71. Saarnio, K.; Teinilä, K.; Saarikoski, S.; Carbone, S.; Gilardoni, S.; Timonen, H.; Aurela, M.; Hillamo, R. Online determination of levoglucosan in ambient aerosols with particle-into-liquid sampler–high-performance anion-exchange chromatography–mass spectrometry (PILS–HPAEC–MS). *Atmos. Meas. Tech.* **2013**, *6*, 2839–2849. [CrossRef]
72. Pérez, N.; Pey, J.; Cusack, M.; Reche, C.; Querol, X.; Alastuey, A.; Viana, M. Variability of Particle Number, Black Carbon, and PM10, PM2.5, and PM1 Levels and Speciation: Influence of Road Traffic Emissions on Urban Air Quality. *Aerosol Sci. Technol.* **2010**, *44*, 487–499. [CrossRef]
73. Kucbel, M.; Corsaro, A.; Švédová, B.; Raclavská, H.; Raclavský, K.; Juchelková, D. Temporal and seasonal variations of black carbon in a highly polluted European city: Apportionment of potential sources and the efect of meteorological conditions. *J. Environ. Manag.* **2017**, *203*, 1178–1189. [CrossRef]
74. Kuzu, S.L.; Yavuz, E.; Akyüz, E.; Saral, A.; Akkoyunlu, B.O.; Özdemir, H.; Demir, G.; Ünal, A. Black carbon and size-segregated elemental carbon, organic carbon compositions in a megacity: A case study for Istanbul. *Air Qual. Atmos. Health* **2020**, *13*, 827–837. [CrossRef]
75. Sharma, R.K.; Bhattarai, B.K.; Sapkota, B.K.; Gewali, M.B.; Kjeldstad, M.B. Black carbon aerosols variation in Kathmandu valley. Nepal. *Atmos. Environ.* **2012**, *63*, 282–288. [CrossRef]
76. Fuller, G.W.; Tremper, A.H.; Baker, T.D.; Yttri, K.E.; Butterfield, D. Contribution of wood burning to PM 10 in London. *Atmos. Environ.* **2014**, *87*, 87–94. [CrossRef]

77. Diapouli, E.; Kalogridis, A.-C.; Markantonaki, C.; Vratolis, S.; Fetfatzis, P.; Colombi, C.; Eleftheriadis, K. Annual Variability of Black Carbon Concentrations Originating from Biomass and Fossil Fuel Combustion for the Suburban Aerosol in Athens, Greece. *Atmosphere* **2017**, *8*, 234. [CrossRef]
78. Martinsson, J.; Abdul Azeem, H.; Sporre, M.K.; Bergström, R.; Ahlberg, E.; Öström, E.; Kristensson, A.; Swietlicki, E.; Eriksson Stenström, K. Carbonaceous aerosol source apportionment using the Aethalometer model–evaluation by radiocarbon and levoglucosan analysis at a rural background site in southern Sweden. *Atmos. Chem. Phys.* **2017**, *17*, 4265–4281. [CrossRef]
79. Pataud, J.P.; Cavalli, F.; Crippa, M. *Long-Term Trends in Black Carbon from Biomass and Fossil Fuel Combustion Detected at the JRC Atmospheric Observatory in Ispra, EUR 29147 EN*; JRC110502; Publications Office of the European Union: Luxembourg, 2018; ISBN 978-92-79-80976-7. [CrossRef]
80. Zheng, H.; Kong, S.; Wu, F.; Cheng, Y.; Niu, Z.; Zheng, S.; Yang, G.; Yao, L.; Yan, Q.; Zheng, M.; et al. Intra-regional transport of black carbon between the south edge of the North China Plain and central China during winter haze episodes. *Atmos. Chem. Phys.* **2019**, *19*, 4499–4516. [CrossRef]
81. Klejnowski, K.; Janoszka, K.; Czaplicka, M. Characterization and Seasonal Variations of Organic and Elemental Carbon and Levoglucosan in PM_{10} in Krynica Zdroj, Poland. *Atmosphere* **2017**, *8*, 190. [CrossRef]
82. Juda-Rezler, K.; Reizer, M.; Oudinet, J.-P. Determination and analysis of PM10 source apportionment during episodes of air pollution in Central Eastern European urban areas: The case of wintertime 2006. *Atmos. Environ.* **2011**, *45*, 6557–6566. [CrossRef]
83. Błaszczak, B.; Rogula-Kozłowska, W.; Mathews, B.; Juda-Rezler, K.; Klejnowski, K.; Rogula-Kopiec, P. Chemical Compositions of PM2.5 at Two Non-Urban Sites from the Polluted Region in Europe. *Aerosol Air Qual. Res.* **2016**, *16*, 2333–2348. [CrossRef]
84. Zhou, X.; Gao, J.; Wang, T.; Wu, W.; Wang, W. Measurement of black carbon aerosols near two Chinese megacities and the implications for improving emission inventories. *Atmos. Environ.* **2009**, *43*, 3918–3924. [CrossRef]
85. Badarinath, K.V.S.; Kumar Kharol, S.; Kiran Chand, T.R.; Parvathi, Y.G.; Anasuya, T.; Jyothsna, A.N. Variations in black carbon aerosol, carbon monoxide and ozone over an urban area of Hyderabad, India, during the forest fire season. *Atmos. Res.* **2017**, *85*, 18–26. [CrossRef]
86. Singh, V.; Ravindra, K.; Sahu, L.; Sokhi, R. Trends of atmospheric black carbon concentration over United Kingdom. *Atmos. Environ.* **2018**, *178*, 148–157. [CrossRef]
87. Kassomenos, P.A.; Vardoulakis, S.; Chaloulakou, A.; Pschalidou, A.K.; Grivas, G.; Borge, R.; Lumbreras, J. Study of PM10 and PM2.5 levels in three European cities: Analysis of intra and inter urban variations. *Atmos. Environ.* **2014**, *87*, 153–163. [CrossRef]
88. Fernandez Gutierrez, M.; Baxter, D.; Hunter, C.; Svoboda, K. Nitrous Oxide (N2O) Emissions from Waste and Biomass to Energy Plants. *Waste Manag. Res.* **2005**, *23*, 133–147. [CrossRef]
89. Cofer, W.R.; Levine, J.S.; Winstead, E.L.; Stocks, B.J. New Estimates of Nitrous Oxide Emissions from Biomass Burning. Available online: https://www.cfs.nrcan.gc.ca/publications?id=38683 (accessed on 14 January 2021).
90. Shen, L.; Li, L.; Lü, S.; Zhang, X.; Liu, J.; An, J.; Zhang, G.; Wu, B.; Wang, F. Characteristics of black carbon aerosol in Jiaxing, China during autumn. *Particuology* **2013**, *20*, 10–15. [CrossRef]
91. Pastuszka, J.S.; Rogula-Kozłowska, W.; Zajusz-Zubek, E. Characterization of PM10 and PM2.5 and associated heavy metals at the crossroads and urban background site in Zabrze, Upper Silesia, Poland, during the smog episodes. *Environ. Monit. Assess.* **2010**, *168*, 613–627. [CrossRef] [PubMed]
92. Rogula-Kozłowska, W.; Błaszczak, B.; Szopa, S.; Klejnowski, K.; Sówka, I.; Zwoździak, A.; Jabłońska, M.; Mathews, B. PM2.5 in the central part of Upper Silesia, Poland: Concentrations, elemental composition, and mobility of components. *Environ. Monit. Assess.* **2013**, *185*, 581–601. [CrossRef]
93. Cheng, Y.-H.; Yun, K.Y.; Jian, L.-J. Correlations between black carbon mass and size-resolved particle number concentrations in the Taipei urban area: A five-year long-term observation. *Atmos. Pollut. Res.* **2014**, *5*, 62–72. [CrossRef]
94. Yang, Q.; Yuan, Q.; Li, T.; Shen, H.; Zhang, L. The Relationship between $PM_{2.5}$ and Meteorological Factors in China: Seasonal and Regional Variations. *Int. J. Environ. Res. Public Health* **2017**, *14*, 1510. [CrossRef]
95. Wang, J.; Ogawa, S. Effects of Meteorological Conditions on $PM_{2.5}$ Concentrations in Nagasaki, Japan. *Int. J. Environ. Res. Public Health* **2015**, *12*, 9089–9101. [CrossRef]
96. Tai, A.P.K.; Mickley, L.J.; Jacob, D.J.; Leibensperger, E.M.; Zhang, L.; Fisher, J.A.; Pye, H.O.T. Meteorological modes of variability for fine particulate matter ($PM_{2.5}$) air quality in the United States: Implications for $PM_{2.5}$ sensitivity to climate change. *Atmos. Chem. Phys.* **2012**, *12*, 3131–3145. [CrossRef]
97. Galindo, N.; Varea, M.; Gil-Moltó, J.; Yubero, E. The Influence of Meteorology on Particulate Matter Concentrations at an Urban Mediterranean Location. *Water Air Soil Pollut.* **2011**, *215*, 365–372. [CrossRef]
98. Heo, J.; McGinnis, J.E.; de Foy, B.; Schauer, J.J. Identification of potential source areas for elevated PM2.5, nitrate and sulfate concentrations. *Atmos. Environ* **2013**, *71*, 187197. [CrossRef]
99. Ragosta, M.; Caggiano, R.; D'Emilio, S.S.; Trippetta, S.; Macchiato, M. PM10and heavy metal measurements in an industrialarea of southern Italy. *Atmos. Res.* **2006**, *81*, 304–319. [CrossRef]
100. Pilguj, N.; Kendzierski, S.; Kolendowicz, L. The role of the atmospheric circulation types on PM_{10} concentrations in Poznań. *Geogr. Overv.* **2018**, *90*, 77–91.
101. European Commission. DG Environment 2010. Guidance on Assessment around Point Sources under the EU Air Quality Directive 2008/50/EC. Available online: https://ec.europa.eu/environment/air/quality/legislation/pdf/Guidance%20on%20assessment%20around%20point%20sources%20AQCincluded_final.pdf (accessed on 14 January 2021).

102. Leśniok, M.R.; Caputa, Z.A. The role of atmospheric circulation in air pollution distribution in Katowice Region (Southern Poland). *Int. J. Environ. Waste Manag.* **2009**, *4*, 62–74. [CrossRef]
103. Pietras, B. Circulation conditions for the presence of high concentrations of particulate matter in Kraków. In *Physiographic Research. Series A—Physical Geography*; Publishing House of the Poznań Society of Friends of Sciences: Kraków, Poland, 2015; Volume 66, pp. 121–130.